

New Coordination Polymers and Supramolecular Complexes Generated from Oxadiazole-Containing Organic Ligands and Inorganic M(II) (M = Zn and Cu) Salts

Yu-Bin Dong,* Jun-Yan Cheng, Huai-You Wang, Ru-Qi Huang, and Bo Tang

College of Chemistry, Chemical Engineering and Materials Science, and Shandong Key Lab of Functional Chemical Materials, Shandong Normal University, Jinan 250014, People's Republic of China

Mark D. Smith and Hans-Conrad zur Loyer

Department of Chemistry and Biochemistry, University of South Carolina, Columbia, South Carolina 29208

Received January 24, 2003. Revised Manuscript Received April 8, 2003

The coordination chemistry of the oxadiazole-containing rigid bidentate ligands 2,5-bis(4-pyridyl)-1,3,4-oxadiazole (L1) and 2,5-bis(3-pyridyl)-1,3,4-oxadiazole (L2) with inorganic M(II) (M = Zn and Cu) salts has been investigated. Two new coordination polymers (**1** and **2**) and two new bimetallic macrocyclic supramolecular complexes (**3** and **4**) were synthesized from solution reactions of L1 and L2 with inorganic M(II) (M = Zn and Cu) salts, respectively. $\{[\text{Zn}(\text{L1})(\text{H}_2\text{O})_2(\text{CH}_3\text{CN})_2](\text{ClO}_4)_2 \cdot (\text{L1})(\text{CH}_3\text{CN})_{1.5}(\text{CH}_2\text{Cl}_2)_{0.5}\}_n$ (**1**; monoclinic, $P2_1/m$, $a = 7.5755(4)$ Å, $b = 8.3120(16)$ Å, $c = 9.6449(6)$ Å, $\beta = 99.9920(10)^\circ$, $Z = 2$) was obtained by combination of L1 with $\text{Zn}(\text{ClO}_4)_2 \cdot 6\text{H}_2\text{O}$ in a $\text{CH}_2\text{Cl}_2/\text{CH}_3\text{CN}$ mixed-solvent system. The structure features one-dimensional chains that are cross-linked to each other by weak noncovalent $\pi-\pi$ interactions (alternating face-to-face stacking of coordinated and uncoordinated L1 molecules) to generate a novel two-dimensional network. $\{[\text{Zn}(\text{L1})(\text{H}_2\text{O})_2(\text{NO}_3)_2] \cdot 2(\text{CH}_3\text{CN})_2\}_n$ (**2**; monoclinic, $C2/c$, $a = 27.2789(18)$ Å, $b = 11.7378(8)$ Å, $c = 7.3357(5)$ Å, $\beta = 101.4270(10)^\circ$, $Z = 4$) was obtained by combination of L1 with $\text{Zn}(\text{NO}_3)_2 \cdot 6\text{H}_2\text{O}$ in the same solvent system. It forms with an unique H-bonded three-dimensional framework that contains rhombic channels (crystallographic dimensions, 18×10 Å²) running down the crystallographic c axis. Inside the channels are double columns of CH_3CN molecules, stacked neatly upon one another. $[\text{Zn}(\text{L2})(\text{H}_2\text{O})_3(\text{NO}_3)_2]_2(\text{NO}_3)_2$ (**3**; monoclinic, $P2_1/c$, $a = 13.8786(7)$ Å, $b = 12.5179(7)$ Å, $c = 9.8966(5)$ Å, $\beta = 97.5790(10)^\circ$, $Z = 2$) and $[\{\text{Cu}(\text{L2})(\text{CH}_3\text{CN})(\text{NO}_3)_2\}_2$ (**4**; triclinic, $\bar{P}1$, $a = 7.7416(5)$ Å, $b = 8.5956(5)$ Å, $c = 13.3020(8)$ Å, $\alpha = 74.3470(10)^\circ$, $\beta = 78.4420(10)^\circ$, $\gamma = 86.2340(10)^\circ$, $Z = 1$) were generated from the reactions of L2 with $\text{Zn}(\text{NO}_3)_2 \cdot 6\text{H}_2\text{O}$ and $\text{Cu}(\text{NO}_3)_2 \cdot 6\text{H}_2\text{O}$ in a $\text{CH}_2\text{Cl}_2/\text{CH}_3\text{CN}$ mixed-solvent system, respectively. Both **3** and **4** adopt a novel bimetallic macrocyclic structural motif, consisting of $\text{M}_2(\text{L2})_2$ (M = Zn and Cu) ringlike units. Hydrogen-bonding interactions in **3** and noncovalent $\pi-\pi$ interactions in **4** play a significant role in aligning the molecular dimeric squares in the solid state. Compounds **3** and **4** are soluble in both water and organic solvents. In addition, both compounds are luminescent in the solid state and a large red shift in the emission is observed between the free ligand L2 and the ligand incorporated into both complexes **3** and **4**.

Introduction

The design and synthesis of functional supramolecular coordination polymers with novel topologies and structural motifs are of current interest in the field of coordination chemistry.^{1,2} Over the past decades, different classes of polymeric compounds fitting this general description have been successfully designed and synthesized. Some of them exhibit encouraging potential for applications, including nonlinear optics, catalysis

and separation, magnetism, molecular recognition, and fluorescent materials.³ In the long run, this line of research can lead to predictions of the topology and/or the periodicity of crystalline lattices generated from the molecular structures of the participating small building blocks; in fact, one can anticipate that the relationship between polymeric structures and physical properties will eventually be elucidated as well. The most efficient approach to access this type of material is via the direct chemical combination of functional inorganic and organic components, as has been demonstrated by many previous studies.^{1,2}

* To whom correspondence should be addressed. E-mail: yubindong@sdnu.edu.cn.

So far, several types of bidentate rigid organodiamine ligands, such as 4,4'-bipyridine,^{4a} 1,2-bis(4-pyridyl)-ethene,^{4b} 1,2-bis(4-pyridyl)ethyne,^{4c} 1,4-bis(3-pyridyl)-2,3-diaza-1,3-butadiene,^{4e} and 2,5-bis(3-pyridyl)-3,4-diaza-2,4-hexadiene,^{4f,g} have been utilized by us as well as by numerous other research groups¹ to construct coordination polymers. All of these bidentate N-donor-containing ligands have proven to be among the most important types of organic ligands for the design and construction of coordination polymers exhibiting remarkable polymeric structural motifs. However, in most cases, the geometries of these bidentate ligands that were used to construct coordination polymers are linear. In other words, the linear bidentate organic spacers are the major theme in the chemistry of coordination polymer and supramolecular complexes. A continuing project in our laboratory has been the development of coordination polymers generated from oxadiazole-containing organic ligands and inorganic salts.⁵ The bridging five-membered oxadiazole ring ensures that the geometries of these ligands are not linear. On the other hand, oxadiazole ring-containing organic spacers are widely used to construct luminescent materials by incorporating them into all-organic or inorganic/organic composite species.^{5,6} As a result of the conjugated bent

(1) (a) Hagrman, P. J.; Hagrman, D.; Zubietta, J. *Angew. Chem., Int. Ed.* **1999**, *38*, 2638. (b) Blake, A. J.; Champness, N. R.; Hubberstey, P.; Li, W.-S.; Withersby, M. A.; Schröder, M. *Coord. Chem. Rev.* **1999**, *183*, 117. (c) Batten, S.; Robson, R. *Angew. Chem., Int. Ed. Engl.* **1998**, *37*, 1460. (d) Yaghi, O. M.; Li, G.; Li, H. *Nature* **1995**, *378*, 703. (e) Yaghi, O. M.; Li, H. *J. Am. Chem. Soc.* **1995**, *117*, 10401. (f) Yaghi, O. M.; Li, H.; Groy, T. L. *J. Am. Chem. Soc.* **1996**, *118*, 9096. (g) Fujita, M.; Oka, H.; Yamaguchi, K.; Ogura, K. *Nature* **1995**, *378*, 469. (h) Fujita, M.; Kwon, Y. J.; Sasaki, O.; Yamaguchi, K.; Ogura, K. *J. Am. Chem. Soc.* **1995**, *117*, 7287. (i) Losier, T. P.; Zaworotko, M. *J. Angew. Chem., Int. Ed. Engl.* **1996**, *35*, 2779. (g) Power, K. N.; Hennigar, L.; Zaworotko, M. *J. Chem. Commun.* **1998**, 595.

(2) (a) Heintz, R. A.; Zhao, H.; Ouyang, X.; Grandinetti, G.; Cowen, J.; Dumbar, K. R. *Inorg. Chem.* **1999**, *38*, 144. (b) Mayr, A.; Guo, J. *Inorg. Chem.* **1999**, *38*, 921. (c) Mayr, A.; Mao, L. F. *Inorg. Chem.* **1998**, *37*, 5776. (d) Mao, L. F.; Mayr, A. *Inorg. Chem.* **1996**, *35*, 3183. (e) Choi, H. J.; Suh, M. P. *J. Am. Chem. Soc.* **1998**, *120*, 10622. (f) Sharma, C. V. K.; Broker, G. A.; Huddleston, J. G.; Baldwin, J. W.; Metzger, R. M.; Rogers, R. D. *J. Am. Chem. Soc.* **1999**, *121*, 1137.

(3) (a) Fujita, M.; Kwon, Y. J.; Washizu, S.; Ogura, K. *J. Am. Chem. Soc.* **1999**, *116*, 1151. (b) Lin, W.; Evans, O. R.; Xiong, R.-G.; Wang, Z. *J. Am. Chem. Soc.* **1998**, *120*, 13272. (c) Garder, G. B.; Venkataraman, D.; Moore, J. S.; Lee, S. *Nature* **1995**, *374*, 792. (d) Garder, G. B.; Kiang, Y.-H.; Lee, S.; Asgaonkar, A.; Venkataraman, D. *J. Am. Chem. Soc.* **1996**, *118*, 6946. (e) Kahn, O.; Pei, Y.; Verduguer, M.; Renard, J. P.; Sletten, J. *J. Am. Chem. Soc.* **1998**, *120*, 782. (f) Inoue, K.; Hayamizu, T.; Iwamura, H.; Hashizume, D.; Ohashi, Y. *J. Am. Chem. Soc.* **1996**, *118*, 1803. (g) Tamaki, H.; Zhong, Z. J.; Matsumoto, N.; Kida, S.; Koikawa, M.; Achiwa, N.; Hashimoto, Y.; Okawa, H. *J. Am. Chem. Soc.* **1992**, *114*, 6974.

(4) (a) Dong, Y.-B.; Smith, M. D.; Layland, R. C.; zur Loya, H.-C. *J. Chem. Soc., Dalton Trans.* **2000**, 775. (b) Dong, Y.-B.; Layland, R. C.; Smith, M. D.; Pschirer, N. G.; Bunz, U. H. F.; zur Loya, H.-C. *Inorg. Chem.* **1999**, *38*, 3056. (c) Dong, Y.-B.; Layland, R. C.; Pschirer, N. G.; Smith, M. D.; Bunz, U. H. F.; zur Loya, H.-C. *Chem. Mater.* **1999**, *11*, 1415. (d) Dong, Y.-B.; Smith, M. D.; Layland, R. C.; zur Loya, H.-C. *Inorg. Chem.* **1999**, *38*, 5027. (e) Dong, Y.-B.; Smith, M. D.; Layland, R. C.; zur Loya, H.-C. *Chem. Mater.* **2000**, *12*, 1156. (f) Dong, Y.-B.; Smith, M. D.; zur Loya, H.-C. *Inorg. Chem.* **2000**, *39*, 4927. (g) Ciurton, D. M.; Dong, Y.-B.; Smith, M. D.; Barclay, T.; zur Loya, H.-C. *Inorg. Chem.* **2001**, *40*, 2825.

(5) (a) Dong, Y.-B.; Ma, J.-P.; Smith, M. D.; Huang, R.-Q.; Tang, B.; Chen, D.; zur Loya, H.-C. *Solid State Sci.* **2002**, *4*, 1313. (b) Dong, Y.-B.; Ma, J.-P.; Huang, R.-Q.; Smith, M. D.; zur Loya, H.-C. *Inorg. Chem.* **2003**, *42*, 294. (c) Dong, Y.-B.; Ma, J.-P.; Smith, M. D.; Huang, R.-Q.; Tang, B.; Guo, D.-S.; Wang, J.-S.; zur Loya, H.-C. *Solid State Sci.* **2003**, *5*, 601–610. (d) Dong, Y.-B.; Cheng, J. Y.; Ma, J.-P.; Wang, H.-Y.; Huang, Y.-Q.; Guo, D.-S.; Smith, M. D. *Solid State Sci.* **2003**, in press.

(6) (a) Lee, D. W.; Kwon, K.-Y.; Jin, J.-I.; Park, Y.; Kim, Y.-R.; Hwang, I.-W. *Chem. Mater.* **2001**, *13*, 565. (b) Wang, J.; Wang, R.; Yang, J.; Zheng, Z.; Carducci, M. D.; Cayou, T.; Peyghambarian, N.; Jabbour, G. E. *J. Am. Chem. Soc.* **2001**, *123*, 6179.

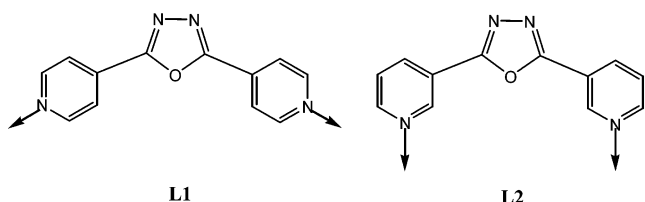


Figure 1. Rigid organic oxadiazole-containing ligands used in the construction of coordination polymer frameworks.

shape of the oxadiazole-containing ligand and the coordination preferences of transition metals, new types of coordination polymers, some with open channels or interesting luminescent properties, have been obtained. Moreover, heteroatoms such as N and O with free electron pairs on the five-membered heterocyclic rings could be considered as potential active coordination sites and/or hydrogen bond acceptors to expand the polymeric frameworks with coordinative covalent bonds and/or hydrogen-bonding interactions.⁵

Herein, we report two new coordination polymers and two new supramolecular bimetallic complexes, namely, $\{[Zn(L1)(H_2O)_2(CH_3CN)_2](ClO_4)_2\} \cdot (L1) \cdot (CH_3CN)_{1.5}(CH_2Cl_2)_{0.5} \cdot n$ (**1**), $\{[Zn(L1)(H_2O)_2(NO_3)_2] \cdot 2(CH_3CN)_2\} \cdot n$ (**2**), $[Zn(L2)(H_2O)_3(NO_3)_2] \cdot (NO_3)_2$ (**3**), and $\{[Cu(L2)(CH_3CN)_2](NO_3)_2\}$ (**4**) based on 1,3,4-oxadiazole-containing ligands **L1** and **L2** (Figure 1) and $M(II)$ -containing [$M(II) = Zn(II)$ and $Cu(II)$] inorganic salts. In addition, the luminescent properties of **L1** and supramolecular complexes **3** and **4** were also reported herein.

Experimental Section

Materials and Methods. Ligands **L1** [2,5-bis(4-pyridyl)-1,3,4-oxadiazole] and **L2** [2,5-bis(3-pyridyl)-1,3,4-oxadiazole] were prepared according to literature methods.⁷ All other solvents and reagents were used as received from commercial sources. Infrared (IR) samples were prepared as KBr pellets, and spectra were obtained in the 400–4000 cm^{-1} range using a Perkin-Elmer 1600 FTIR spectrometer. Elemental analyses were performed on a Perkin-Elmer model 2400 analyzer.

Caution! One of the crystallization procedures involves $Zn(ClO_4)_2 \cdot 6H_2O$, which is a strong oxidizer.

Preparation of $\{[Zn(L1)(H_2O)_2(CH_3CN)_2](ClO_4)_2\} \cdot (L1) \cdot (CH_3CN)_{1.5}(CH_2Cl_2)_{0.5} \cdot n$ (1**)**. A solution of $Zn(ClO_4)_2 \cdot 6H_2O$ (37.2 mg, 0.10 mmol) in CH_3CN (8 mL) was layered onto a solution of **L1** (22.4 mg, 0.10 mmol) in methylene chloride (8 mL). The solutions were left for about 1 week at room temperature, and colorless crystals were obtained. Yield: 68% [based on $Zn(ClO_4)_2 \cdot 6H_2O$]. Anal. Calcd for $ZnC_{31.5}H_{31.5}N_{11.5}O_{12} \cdot Cl_3$ (**1**): C, 40.43; H, 3.37; N, 17.22. Found: C, 40.56; H, 3.41; N, 17.19. IR (KBr, cm^{-1}): 3510(br), 3150(s), 1673(m), 1629(s), 1574(s), 1547(s), 1490(s), 1430(s), 1340(w), 1285(m), 1220(w), 1120(vs), 1100(vs), 1010(w), 840(s), 710(s).

Preparation of $\{[Zn(L1)(H_2O)_2(NO_3)_2] \cdot 2(CH_3CN)_2\} \cdot n$ (2**)**. A solution of $Zn(NO_3)_2 \cdot 6H_2O$ (29.7 mg, 0.10 mmol) in CH_3CN (8 mL) was layered onto a solution of **L1** (22.4 mg, 0.10 mmol) in methylene chloride (8 mL). The solutions were left for about 2 weeks at room temperature, and colorless crystals were obtained. Yield: 62% [based on $Zn(NO_3)_2 \cdot 6H_2O$]. Anal. Calcd for $ZnC_{16}H_{18}N_8O_9$ (**2**): C, 36.11; H, 3.39; N, 21.06. Found: C, 36.21; H, 3.40; N, 21.12. IR (KBr, cm^{-1}): 3400(br), 1667(m), 1622(s), 1589(w), 1570(w), 1555(m), 1490(s), 1472(w), 1385(vs), 1340(vs), 1326(vs), 1200(m), 1130(w), 1108(m), 1056(m), 1040(w), 1007(w), 965(w), 815(s), 730(s), 690(s).

Preparation of $[Zn(L2)(H_2O)_3(NO_3)_2] \cdot (NO_3)_2$ (3**)**. A solution of $Zn(NO_3)_2 \cdot 6H_2O$ (29.7 mg, 0.10 mmol) in CH_3CN (8 mL) was layered onto a solution of **L2** (22.4 mg, 0.10 mmol) in methylene chloride (8 mL). The solutions were left for about

Table 1. Crystallographic Data for **1 and **2****

empirical formula	C _{31.50} H _{31.50} Cl ₃ N _{11.50} O ₁₂ Zn (1)	C ₁₆ H ₁₈ N ₈ O ₉ Zn (2)
fw	934.90	531.75
cryst syst	monoclinic	monoclinic
<i>a</i> (Å)	7.5755(4)	27.2789(18)
<i>b</i> (Å)	28.3120(16)	11.7378(8)
<i>c</i> (Å)	9.6449(6)	7.3357(5)
α (deg)	90	90
β (deg)	99.9920(10)	101.4270(10)
γ (deg)	90	90
<i>V</i> (Å ³)	2037.2(2)	2302.3(3)
space group	<i>P</i> 2 ₁ / <i>m</i>	<i>C</i> 2/ <i>c</i>
<i>Z</i> value	2	4
ρ(calcd) (g/cm ³)	1.524	1.534
μ(Mo Kα) (cm ⁻¹)	11.258	11.329
temp (K)	150	150
no. of obsns (<i>I</i> > 3σ)	3683	2371
residuals: <i>R</i> ; <i>R</i> _w	0.067; 0.1253	0.0379; 0.0797

^a $R = \sum |F_o| - |F_c|/|\sum F_o|$. $wR = \{\sum [w(F_o^2 - F_c^2)^2]/\sum [w(F_o^2)^2]\}^{1/2}$.

2 weeks at room temperature, and colorless crystals were obtained. Yield: 85% [based on Zn(NO₃)₂·6H₂O]. Anal. Calcd for Zn₂C₂₄H₂₈N₁₂O₂₀: C, 30.79; H, 2.99; N, 17.96. Found: C, 30.78; H, 3.01; N, 17.78. IR (KBr, cm⁻¹): 3400(br), 1667(m), 1622(s), 1589(w), 1570(w), 1555(w), 1490(m), 1472(w), 1410(vs), 1385(vs), 1340(vs), 1326(vs), 1200(m), 1130(w), 1108(m), 1056(m), 1040(w), 1007(w), 965(w), 815(s), 730(s), 690(s).

Preparation of $[\text{Cu}(\text{L}2)(\text{CH}_3\text{CN})(\text{NO}_3)_2$ (4). A solution of Cu(NO₃)₂·6H₂O (24.1 mg, 0.10 mmol) in CH₃CN (8 mL) was layered onto a solution of L2 (22.4 mg, 0.10 mmol) in methylene chloride (8 mL). The solutions were left for about 2 weeks at room temperature, and deep-blue crystals were obtained. Yield: 72% [based on Cu(NO₃)₂·6H₂O]. Anal. Calcd for Cu₂C₂₈H₂₂N₁₄O₁₄ (1): C, 37.10; H, 2.43; N, 21.64. Found: C, 37.09; H, 2.45; N, 21.55. IR (KBr, cm⁻¹): 2291(w), 1620(s), 1595(w), 1550(m), 1480(s), 1445(s), 1420(s), 1388(s), 1295(s), 1265(s), 1195(w), 1132(w), 1088(w), 1056(m), 1020(m), 965(w), 820(m), 800(m), 729(s), 628(s).

Single-Crystal Structure Determination. Suitable single crystals of **1–4** were selected and mounted onto the end of thin glass fibers using inert oil. X-ray intensity data were measured at 150 K on a Bruker SMART APEX CCD-based diffractometer (Mo Kα radiation, $\lambda = 0.71073$ Å). The raw frame data for **1–4** were integrated into SHELX-format reflection files and corrected for Lorentz and polarization effects using SAINT.⁸ Corrections for incident and diffracted beam absorption effects were applied using SADABS.⁸ None of the crystals showed evidence of crystal decay during data collection. All structures were solved by a combination of direct methods and difference Fourier syntheses and refined against F^2 by the full-matrix least-squares technique. Crystal data, data collection parameters, and refinement statistics for **1–4** are listed in Tables 1 and 2. Relevant interatomic bond distances and bond angles for **1–4** are given in Tables 3–6.

Results and Discussion

Ligands and Synthesis of Compounds **1–4**.

Ligands L1 and L2 were chosen as simple yet interesting *N,N*-bipyridine-type linkers to investigate their presumed conformational flexibility. Compared to previous linear rigid bidentate ligands,¹ L1 and L2 have distinct geometries and orientations of their coordination sites, which can be considered as modified versions of linear rigid bidentate ligands. This type of ligand might bind metal ions to generate polymeric frameworks or supramolecular architectures with novel topologies that are not achievable to linear rigid *N,N*-bipyridine

Table 2. Crystallographic Data for **3 and **4****

empirical formula	C ₂₄ H ₂₈ N ₁₂ O ₂₀ Zn ₂ (3)	C ₂₈ H ₂₂ Cu ₂ N ₁₄ O ₁₄ (4)
fw	935.32	905.68
cryst syst	monoclinic	triclinic
<i>a</i> (Å)	13.8786(7)	7.7416(5)
<i>b</i> (Å)	12.5179(7)	8.5956(5)
<i>c</i> (Å)	9.8966(5)	13.3020(8)
α (deg)	90	74.3470(10)
β (deg)	97.5790(10)	78.4420(10)
γ (deg)	90	86.2340(10)
<i>V</i> (Å ³)	1704.33(15)	834.99(9)
space group	<i>P</i> 2 ₁ / <i>c</i>	<i>P</i> 1
<i>Z</i> value	2	1
ρ(calcd) (g/cm ³)	1.823	1.801
μ(Mo Kα) (cm ⁻¹)	11.258	11.329
temp (K)	150	150
no. of obsns (<i>I</i> > 3σ)	4221	3398
residuals: <i>R</i> ; <i>R</i> _w	0.0279; 0.0635	0.0379; 0.0762

^a $R = \sum |F_o| - |F_c|/|\sum F_o|$. $wR = \{\sum [w(F_o^2 - F_c^2)^2]/\sum [w(F_o^2)^2]\}^{1/2}$.

Table 3. Interatomic Distances (Å) and Bond Angles (deg) with Estimated Standard Deviations in Parentheses for **1^a**

Zn–O(3)	2.067(3)	Zn–N(1)	2.153(2)
Zn–N(5)	2.179(2)		
O(3) ^{#1} –Zn–O(3)	180.000(1)	O(3) ^{#1} –Zn–N(1)	89.37(10)
N(1)–Zn–N(1) ^{#1}	180.00(14)	O(3)–Zn–N(5)	89.41(11)
N(1)–Zn–N(5)	90.63(10)	N(1)–Zn–N(5) ^{#1}	89.37(10)

^a Symmetry transformations used to generate equivalent atoms: #1, $-x, -y + 1, -z + 1$; #2, $x, -y + 1/2, z$; #3, $x, -y + 3/2, z$.

Table 4. Interatomic Distances (Å) and Bond Angles (deg) with Estimated Standard Deviations in Parentheses for **2^a**

Zn–O(2)	2.0728(14)	Zn–N(1)	2.1350(16)
Zn–O(3)	2.1487(13)		
O(2) ^{#1} –Zn–O(2)	180.0	O(2) ^{#1} –Zn–N(1) ^{#1}	87.81(6)
N(1) ^{#1} –Zn–N(1)	180.00(5)	O(2) ^{#1} –Zn–O(3)	81.37(6)
N(1) ^{#1} –Zn–O(3)	94.03(6)	O(2) ^{#1} –Zn–O(3) ^{#1}	98.63(6)

^a Symmetry transformations used to generate equivalent atoms: #1, $-x + 1/2, -y + 3/2, -z$; #2, $-x + 1, y, -z + 1/2$.

Table 5. Interatomic Distances (Å) and Bond Angles (deg) with Estimated Standard Deviations in Parentheses for **3^a**

Zn–O(3)	2.0759(11)	Zn–O(4)	2.0783(11)
Zn–O(2)	2.0994(11)	Zn–N(4) ^{#1}	2.1176(12)
Zn–N(1)	2.1355(12)	Zn–O(5)	2.2423(10)
O(4)–Zn–O(2)	177.14(4)	N(4) ^{#1} –Zn–N(1)	173.49(4)
O(3)–Zn–O(5)	175.84(4)	O(4)–Zn–O(5)	87.38(4)

^a Symmetry transformations used to generate equivalent atoms: #1, $x + 1, y, z + 1$; #2, $-x + 1, -y + 1, -z + 1$; #3, $x - 1, y, z - 1$.

ligands. In addition, heteroatoms such as N and O on the 1,3,4-oxadiazole ring could be considered as potential hydrogen bond acceptors to expand polymeric frameworks with hydrogen-bonding interactions. L1 and L2 are very soluble in common polar organic solvents such as CH₂Cl₂, CHCl₃, THF, CH₃OH, and C₂H₅OH, which facilitates the solution reaction between the ligands and inorganic metal salts.

The coordination behaviors of L1 and L2 are, however, different. Compounds **1** and **2** were obtained as polymeric compounds by combination of L1 with inorganic M(II) salts. In contrast, compounds **3** and **4** were obtained as supramolecular complexes based on H-bonding and π – π stacking interactions by combination

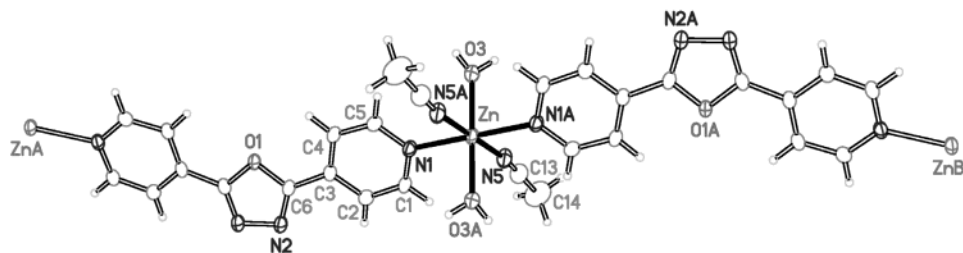


Figure 2. ORTEP figure of **1** with 50% probability ellipsoids.

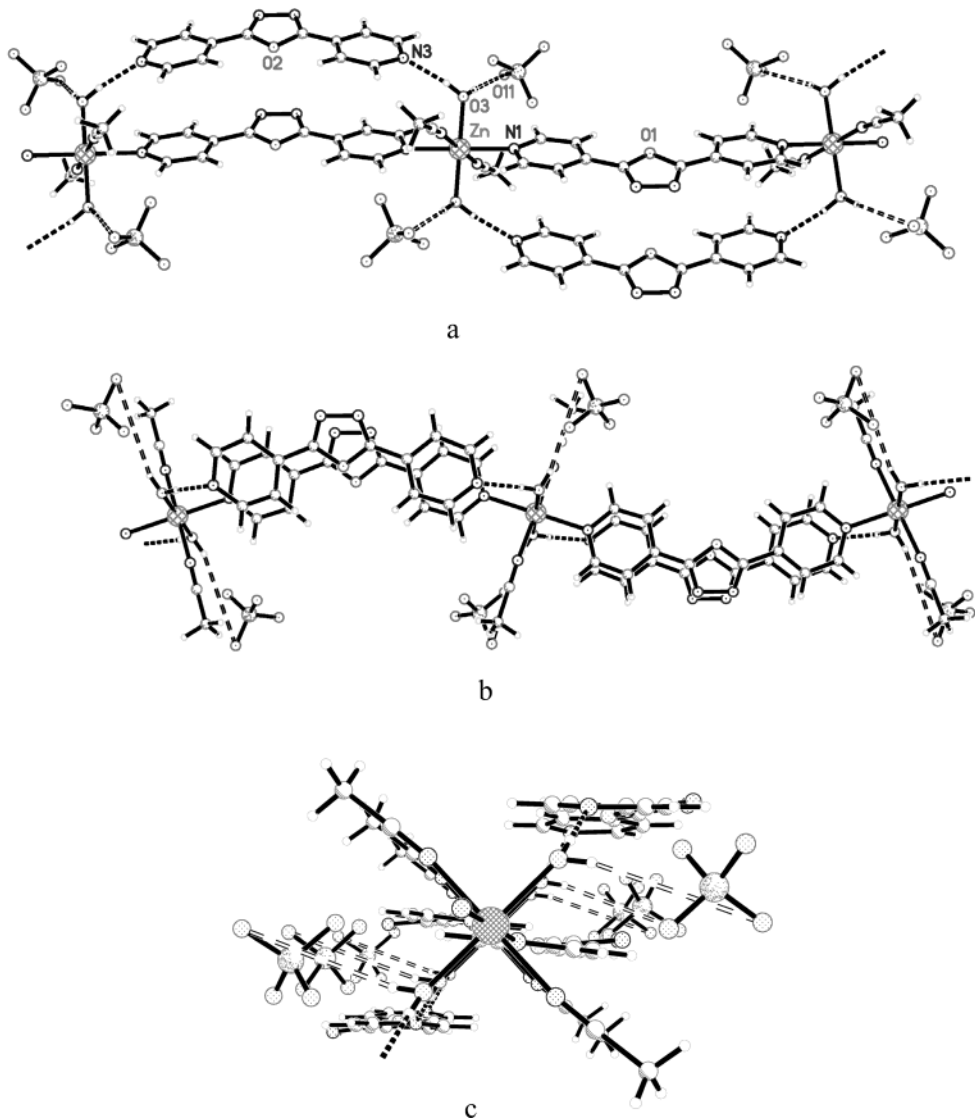


Figure 3. Infinite one-dimensional chains incorporating an additional L1 ligand and the ClO_4^- anion via hydrogen bonds: (a) view down the *c* axis; (b) view down the *a* axis; (c) view down the *b* axis.

of L2 with inorganic M(II) salts. It is worthwhile to point out that, in these specific reactions, the products do not depend on the ligand-to-metal ratio. However, increasing the ligand-to-metal ratio resulted in a somewhat higher yield and higher crystal quality.

Structural Analysis

1. Polymeric Compounds. *Structural Analysis of $\{[\text{Zn}(\text{L1})(\text{H}_2\text{O})_2(\text{CH}_3\text{CN})_2](\text{ClO}_4)_2\}(\text{L1})(\text{CH}_3\text{CN})_{1.5}(\text{CH}_2\text{Cl}_2)_{0.5}\}_n$ (1).* Crystallization of L1 with $\text{Zn}(\text{ClO}_4)_2 \cdot 6\text{H}_2\text{O}$ in $\text{CH}_3\text{CN}/\text{CH}_2\text{Cl}_2$ at room temperature afforded the infinite one-dimensional polymeric compound (**1**) in 68%

Table 6. Interatomic Distances (Å) and Bond Angles (deg) with Estimated Standard Deviations in Parentheses for **4^a**

Cu–O(5)	1.9719(16)	Cu–O(3)	1.9859(16)
Cu–N(1)	2.0188(18)	Cu–N(4) ^{#1}	2.0214(18)
Cu–O(2)	2.5394(17)	Cu–O(6)	2.7439(17)
O(5)–Cu–O(3)	176.40(6)	O(5)–Cu–N(1)	90.58(7)
O(3)–Cu–N(4) ^{#1}	86.95(7)	N(1)–Cu–N(4) ^{#1}	176.37(7)

^a Symmetry transformations used to generate equivalent atoms: ^{#1}, $-x + 1, -y, -z + 1$.

yield. Crystals of **1** lose solvent molecules and turn opaque within several minutes under ambient atmo-

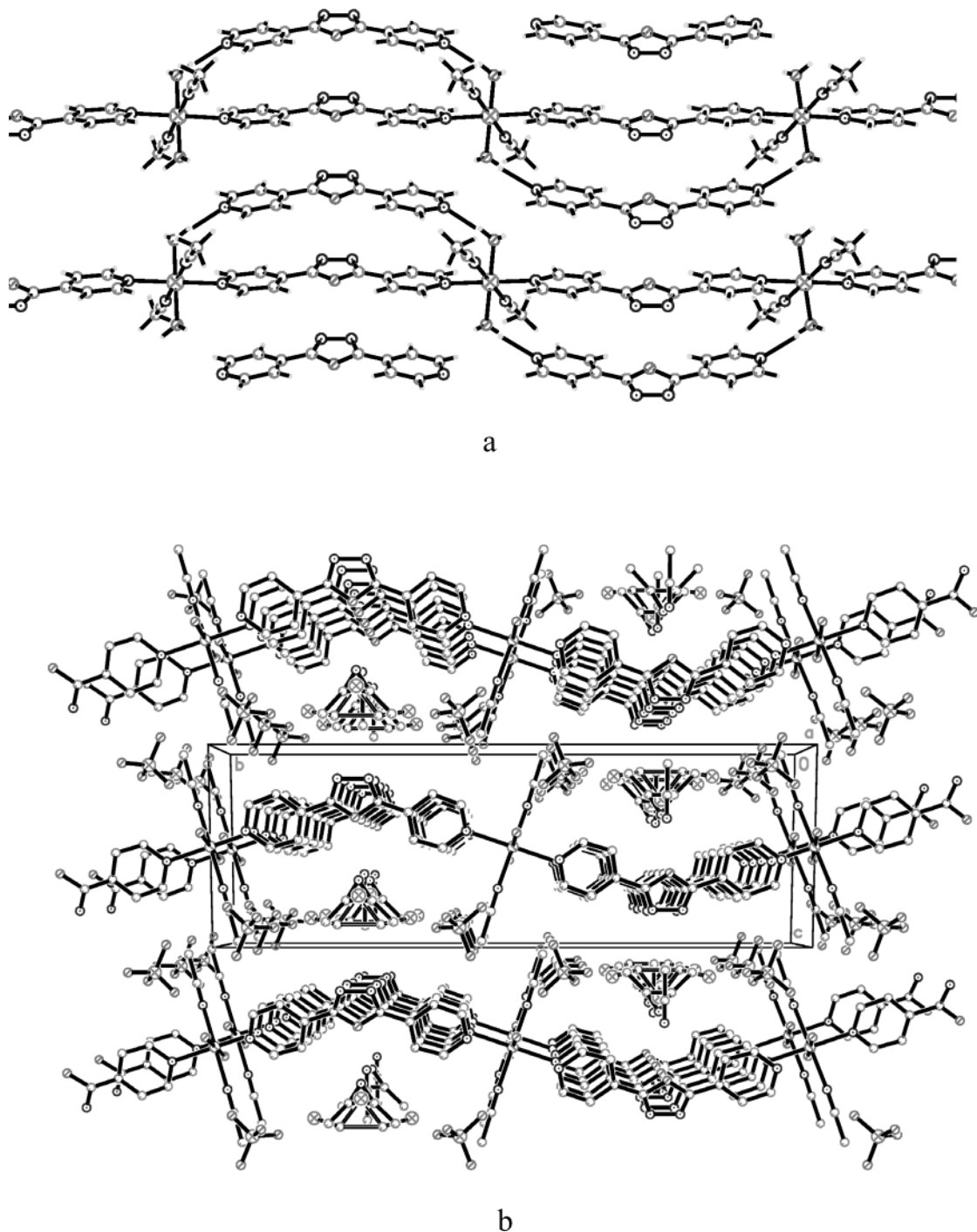


Figure 4. Crystal packing of **1** (two-dimnesional $\pi-\pi$ sheets): (a) view down the *c* axis; (b) view down the *a* axis.

sphere. Single-crystal analysis revealed, as shown in Figure 2, that the coordination sphere of each Zn(II) metal center is defined by four nitrogen donors from two bridged L1 ligands, two nitrogen donors from two terminally coordinated CH_3CN solvent molecules, and two oxygen donors from two coordinated water molecules. The coordination geometry can be described as a basal plane consisting of the trans nitrogen donors $\text{N}(1) \times 2$ and $\text{N}(5) \times 2$, with $\text{Zn}-\text{N}$ distances of 2.153(2) and 2.179(3) Å, respectively. The axial positions are occupied by two oxygen donors $\text{O}(3)$, with a $\text{Zn}-\text{O}$ distance of 2.067(3) Å. All of these bond distances are consistent with the corresponding bond lengths in similar coordination compounds, for example, $[\text{Zn-}$

$(\text{bipyridine})_2\text{SiF}_6 \cdot 2\text{H}_2\text{O}^9$ and $[\text{Zn}(\text{H}_2\text{O})(\text{bipyridine})(\text{NO}_3)_2] \cdot 4,4'\text{-bipyridine}^{10}$. It is worth pointing out that the individual L1 ligands present in **1** are planar; i.e., the two pyridyl donor groups and the bridging oxadiazole ring of each ligand are not rotated with respect to one another.

In the solid state, compound **1** adopts a one-dimensional chain motif, with the Zn(II) centers linked together via two crystallographically equivalent L1 ligands into a one-dimensional chain running along the

(9) Gable, R. W.; Hoskins, B. F.; Robson, R. *J. Chem. Soc., Chem. Commun.* **1990**, 1677.

(10) Carlucci, L.; Ciani, G.; Proserpio, D. M.; Sironi, A. *J. Chem. Soc., Dalton Trans.* **1997**, 1801.

crystallographic *b* axis (Figure 3). These one-dimensional chains are undulating instead of linear because of the bent geometry of the L1 ligand, which is distinctly different from the linear one-dimensional chains found in $[\text{Zn}(\text{H}_2\text{O})(\text{bipyridine})(\text{NO}_3)_2] \cdot 4,4'\text{-bipyridine}$, $[\text{Zn}(\text{H}_2\text{O})_4(\text{bipyridine})](\text{NO}_3)_2 \cdot 2(4,4'\text{-bipyridine}) \cdot 3\text{H}_2\text{O}$, and $[\text{Zn}(\text{H}_2\text{O})_4(\text{bipyridine})][\text{SO}_3\text{CF}_3]_2 \cdot 2(4,4'\text{-bipyridine})$.¹⁰ Two crystallographically equivalent noncoordinated ClO_4^- counterions, as indicated in Figure 3, are located above and below the one-dimensional chains and hydrogen bond to two coordinated water molecules [$\text{O}(11) \cdots \text{O}(3) = 2.836(4)$ and $\text{O}(11) \cdots \text{H}(3\text{B}) = 2.036(3)$ Å, $\text{O}(3) - \text{H}(3\text{B}) \cdots \text{O}(11) = 164(4)^\circ$]. The intrachain and interchain $\text{Zn} \cdots \text{Zn}$ contacts are $14.156(3)$ and $7.57(3)$ Å, respectively. The most important feature in **1** is that there is one (per formula) uncoordinated, crystallographically independent L1 spacer located above and below the one-dimensional chains and hydrogen bonded to two coordinated water molecules [$d_{\text{H}(3\text{A}) \cdots \text{N}(3)} = 1.91(2)$ Å, $d_{\text{O}(3) \cdots \text{N}(3)} = 2.731(4)$ Å, and $\angle \text{O}(3) - \text{H}(3\text{A}) \cdots \text{N}(3) = 172(3)^\circ$; Figure 3]. In addition, the uncoordinated L1 spacers stack with the coordinated L1 ligands in an offset fashion via weak noncovalent $\pi - \pi$ interactions ($d_{\pi - \pi} = 3.70$ Å) along the crystallographic *a* axis (perpendicular to the chains; see Figure 4). Even such weak $\pi - \pi$ interactions, however, serve as important driving forces to cross-link the one-dimensional chains into a novel two-dimensional network running along the crystallographic *a* axis. The disordered CH_3CN and CH_2Cl_2 guest molecules are located between these layers. The participation of bidentate organic spacers such as 4,4'-bipyridine and 1,2-bis(4-pyridyl)ethane in the formation of polymeric frameworks by both coordination and hydrogen bonding interactions is common.^{11,12} Sometimes, weak hydrogen-bonding connectors are effective in extending the dimensions of the network.¹⁰ Some examples have shown that the organic ligands involved (presumably) in the nucleation process use both coordination and $\pi - \pi$ interactions to construct the framework, especially in some porphyrin-containing compounds.¹³ In compound **1**, the free L1 organic spacers do play a critical role in the formation of a $\pi - \pi$ stacking system and, moreover, serve as the agent that allows $\pi - \pi$ interactions to expand the dimensionality of **1** from one to two. Taken all together, almost every type of bonding motif can be found in **1**, including coordination bonding, covalent bonding, hydrogen bonding, and $\pi - \pi$ stacking interactions.

*Structural Analysis of $\{[\text{Zn}(\text{L1})(\text{H}_2\text{O})_2(\text{NO}_3)_2] \cdot 2(\text{CH}_3\text{CN})_2\}_n$ (**2**)*. Crystallization of L1 with $\text{Zn}(\text{NO}_3)_2 \cdot 6\text{H}_2\text{O}$ in $\text{CH}_3\text{CN}/\text{CH}_2\text{Cl}_2$ at room temperature afforded the infinite one-dimensional polymeric compound **2** in 62% yield. Compound **2**, also, is not air stable. As shown in Figure 5, the Zn(II) metal ion lies in a distorted octahedral coordination environment that consists of

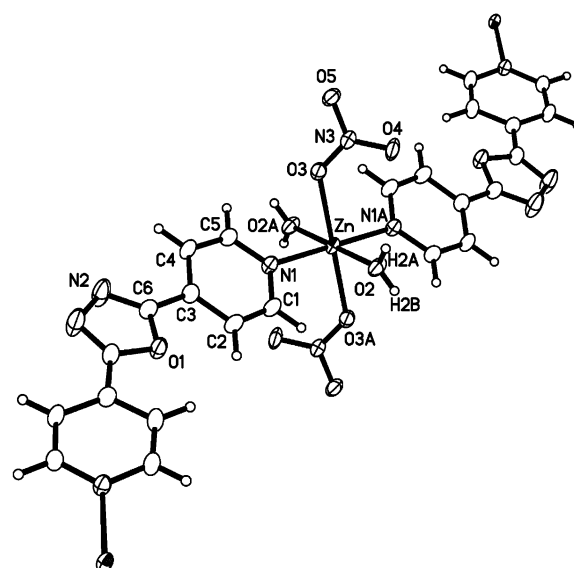


Figure 5. Zn(II) coordination environment in **2** with 50% probability displacement ellipsoids. The Zn(II) ion is located on an inversion center and L1 on a 2-fold axis.

two pyridyl N donors from two L1 ligands, two O donors from two coordinated water molecules, and two O donors from two monodentate NO_3^- counterions. The $\text{Zn} - \text{N}$ and $\text{Zn} - \text{O}_{\text{aquo}}$ bond distances are $2.135(16)$ and $2.0728(14)$ Å, respectively, which are similar to the corresponding bond lengths found in **1**. The $\text{Zn} - \text{O}_{\text{nitrate}}$ bond length is $2.1487(16)$ Å, which is slightly longer than the $\text{Zn} - \text{O}_{\text{aquo}}$ bond distance but is equivalent to the corresponding bond length found in $\text{Zn}_2(\text{BTC})(\text{NO}_3) \cdot (\text{H}_2\text{O}) \cdot (\text{C}_2\text{H}_5\text{OH})_2$.¹⁴

In the solid state, the Zn(II) metal centers are linked together by the pyridyl N donors on the L1 ligands into a one-dimensional sinusoidal chain running along the crystallographic [101] direction (Figure 6). The intra-chain $\text{Zn} \cdots \text{Zn}$ contact is $13.40(3)$ Å, which is slightly shorter than the corresponding distance found in **1**. The pyridyl rings in each L1 ligand are rotated around 8° from coplanarity relative to each other. A very complicated hydrogen bonding system was found in **2**. The corresponding H-bond data are listed in Table 7. As shown in Figure 7, these one-dimensional chains pack together with three sets of hydrogen bonds [$\text{O}(2) - \text{H}(2\text{B}) \cdots \text{O}(5)\#3$, $\text{O}(2) - \text{H}(2\text{A}) \cdots \text{N}(3)\#4$, and $\text{O}(2) - \text{H}(2\text{A}) \cdots \text{O}(5)\#4$] into a novel H-bonded three-dimensional network that leaves rhombic channels (crystallographic dimensions, 18×10 Å²) running down the crystallographic *c* axis. Inside the channels there are double columns of CH_3CN molecules, stacked neatly upon one another (Figure 8). The packing diagram of CH_3CN guest molecules is shown in Figure 9. Interestingly, no bonding interactions are observed between the CH_3CN guest molecules and the framework.

Extended networks assembled by both coordination and hydrogen bonds now are well established.^{5a,10} In principle, higher dimensionality networks can be obtained by the assembly of lower dimensionality polymers (or molecules) via hydrogen-bonding interactions. A series of such compounds, namely, $[\text{Zn}(\text{H}_2\text{O})(\text{bipy})] \cdot (\text{NO}_3)_2\text{-bipy}$, $[\text{Zn}(\text{H}_2\text{O})_4(\text{bipy})](\text{NO}_3)_2 \cdot 2\text{bipy}$, $[\text{Zn}(\text{H}_2\text{O})_4$ -

(11) (a) Sharma, C. V. K.; Rogers, R. D. *Chem. Commun.* **1998**, 1083. (b) Goodgame, D. M. L.; Menzer, S.; Smith, A. M.; Williams, D. J. *Chem. Commun.* **1997**, 339.

(12) (a) Munno, G. D.; Armentano, D.; Poerio, T.; Julve, M.; Real, J. A. *J. Chem. Soc., Dalton Trans.* **1999**, 1813. (b) Moliner, N.; Real, J. A.; Munoz, M. C.; Martinez-Manez, R.; Juan, J. M. C. *J. Chem. Soc., Dalton Trans.* **1999**, 1375.

(13) Gardberg, A. S.; Yang, S.; Hoffman, B. M.; Ibers, J. A. *Inorg. Chem.* **2002**, *41*, 1778. (b) Hunter, C. A.; Sanders, J. K. M. *J. Am. Chem. Soc.* **1990**, *112*, 5525. (c) Hunter, C. A.; Hyde, R. H. *Angew. Chem., Int. Ed. Engl.* **1996**, *35*, 1936.

(14) Yaghi, O. M.; Davis, C. E.; Li, G.; Li, H. *J. Am. Chem. Soc.* **1997**, *119*, 2861.

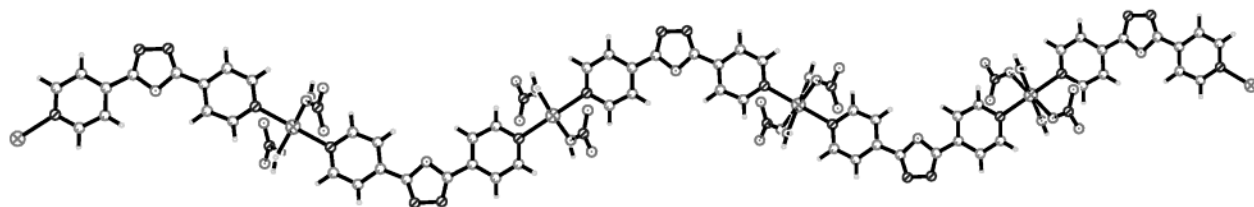


Figure 6. One-dimensional sinusoidal chain of **2** running along [101].

Table 7. Hydrogen Bonds for **2 [Å and deg]^a**

D-H···A	<i>d</i> (D-H)	<i>d</i> (H···A)	<i>d</i> (D···A)	\angle (DHA)
O(2)-H(2B)···O(5) ^{#3}	0.79(2)	1.97(2)	2.7546(19)	175(3)
O(2)-H(2A)···N(3) ^{#4}	0.82(2)	2.73(2)	3.535(2)	169(2)
O(2)-H(2A)···O(5) ^{#4}	0.82(2)	1.93(2)	2.728(2)	166(2)

^a Symmetry transformations used to generate equivalent atoms: #1, $-x + \frac{1}{2}, -y + \frac{3}{2}, -z$; #2, $-x + 1, y, -z + \frac{1}{2}$; #3, $-x + \frac{1}{2}, y + \frac{1}{2}, -z + \frac{1}{2}$; #4, $-x + \frac{1}{2}, -y + \frac{3}{2}, -z + 1$.

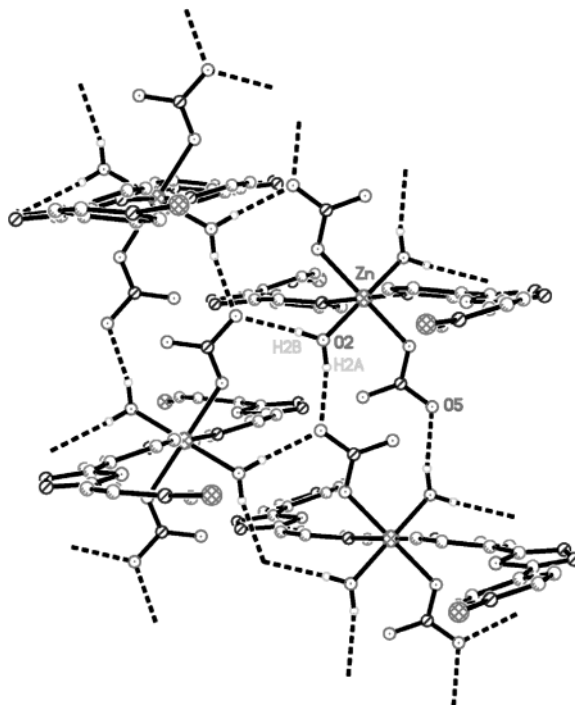


Figure 7. Detail of the three-dimensional hydrogen bonding between the chains in **2**.

(bipy)][SO₃CF₃]₂·2bipy, and Fe(H₂O)₃(ClO₄)(bipy)][ClO₄]·1.5(bipy)·H₂O, were reported before.¹⁰ The extended frameworks of these compounds are based on the one-dimensional [M(bipy)]_n (M = Zn, Fe) linear chains which are cross-linked to each other by M(H₂O)···bipy···H₂O-M hydrogen bond bridges to produce two- and three-dimensional networks. Compounds **1** and **2** reported herein represent additional examples for this kind of compound.

2. Supramolecular Complexes. The idea behind the use of ligand L2 is to control supramolecular motifs through a 3,3'-bipyridine-type ligand.^{6a} It is well-known that the relative orientations of the nitrogen donors on the pyridyl rings and also the different bridging spacing might result in unusual building blocks, which can lead to the construction of supramolecular motifs that have not been achieved using normal rigid linear bidentate organic ligands. We earlier reported on a series of novel coordination polymers generated from rigid bidentate 4,4'-bipyridine- and 3,3'-bipyridine-type Schiff-base

ligands.^{5e-g} Indeed, our previous studies demonstrated that the relative orientations of the coordinating sites are one of the most important factors to control the polymeric motifs.

Structural Analysis of [Zn(L2)(H₂O)₃(NO₃)₂]·(NO₃)₂ (3**) and {Cu(L2)(CH₃CN)(NO₃)₂} (**4**).** Crystallization of L2 with Zn(NO₃)₂·6H₂O in CH₃CN/CH₂Cl₂ at room temperature afforded a dimeric molecular square instead of a polymeric compound due to the different orientations of two pyridyl N donors on an L2 ligand. As shown in Figure 10, the Zn(II) metal center lies in a distorted octahedral coordination environment which is defined by two pyridyl N donors [Zn-N(1) = 2.1355(12) Å and Zn-N(4)^{#1} = 2.1176(12) Å] from two L2 ligands, three O donors [Zn-O(2) = 2.0994(11) Å, Zn-O(3) = 2.0759(11) Å, Zn-O(4) = 2.0783(11) Å] from three coordinated water molecules, and one O donor from one monodentate NO₃⁻ [Zn-O(5) = 2.2423(10) Å]. The bond angle of N(1)-Zn-N(4)^{#1} is 173.49(4)^o, which is not a significant departure from linearity. Two monodentate nitrate counterions are located above and below the macrocycle plane (crystallographic dimensions, 7.6 × 7.7 Å²) and are hydrogen bonded to two coordinated water molecules [O(5)] on the other Zn(II) center. The remaining two nitrate counterions are uncoordinated but hydrogen bonded to two coordinated water molecules [O(4)]. The corresponding hydrogen bond data are listed in Table 8.

In the solid state, these dimeric macrocycles are bonded together by three sets of strong H-bonding interactions, consisting of two coordinated water molecules [O(3) and O(4)] and two free nitrate [O(9) and O(10)] counterions, into a novel three-dimensional H-bonded network. Related hydrogen bond data are listed in Table 8. As shown in Figure 11, the three-dimensional network consists of a porous structure with three different dimensional channels. Their crystallographic dimensions are ca. 9.6 × 3.0, 10.1 × 3.0, and 13.9 × 5.4 Å², respectively. However, no guest solvent molecules are located inside. Networks assembled from mono- or polynuclear metal complexes via hydrogen-bonding interactions are well established.^{5a,15} For example, the materials bis(3-aldoximepyridine)silver(I) hexafluorophosphate, bis(3-aldoximepyridine)silver(I) perchlorate, bis(3-acetylloximepyridine)silver(I) hexafluorophosphate, and bis(3-acetylloximepyridine)silver(I) perchlorate represent an attractive group of two-dimensional architectures formed by the combination of pyridine-oxime ligands with silver(I) salts.¹⁵ We earlier reported a hydrogen-bonded two-dimensional network that consists of "H-shaped" dimetallic Cd₂(H₂O)₄(bipy)₅(NO₃)₂(PF₆)₂ building block molecules linked by intermolecular

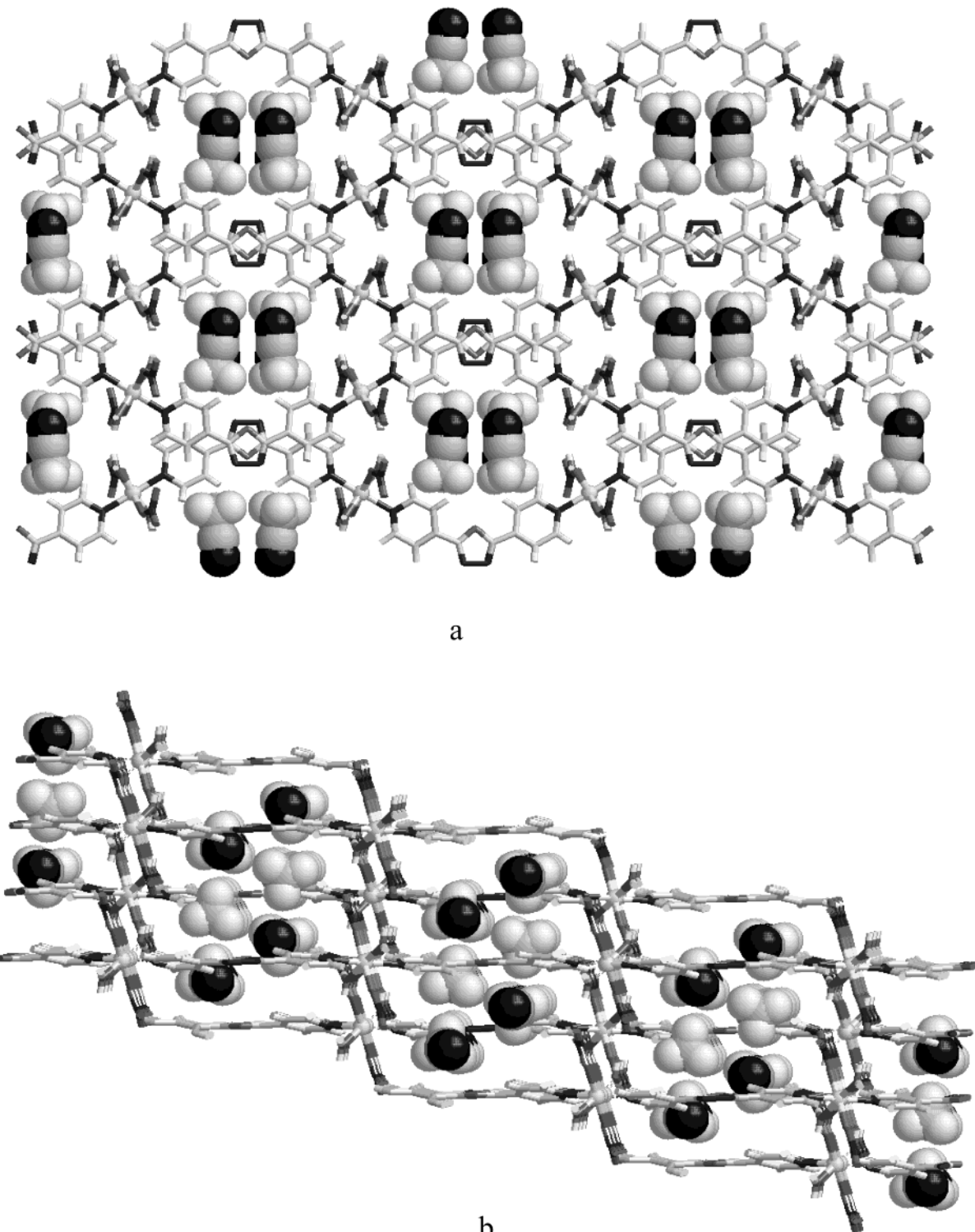


Figure 8. (a) H-bonded three-dimensional network of **2** (view down the *c* axis). Stacks of CH_3CN guests shown with space-filling radii. (b) H-bonded three-dimensional network of **2** (view down the *b* axis).

O–H \cdots N hydrogen bonds.^{5a} So far, high-dimensional H-bonded networks based on bimetallic macrocycle building blocks are still uncommon.

To confirm the universality of the above novel reaction, $\text{Cu}(\text{NO}_3)_2 \cdot 6\text{H}_2\text{O}$ was used instead of $\text{Zn}(\text{NO}_3)_2 \cdot 6\text{H}_2\text{O}$ to carry out the same reaction under the same reaction conditions. Compound **4** was obtained as the same molecular bimetallic macrocycle as **3**. As shown in Figure 12, each Cu(II) center adopts a $\{\text{CuN}_3\text{O}_3\}$ distorted octahedral coordination environment as a

result of the usual copper Jahn–Teller effect. The distorted $4 + 2$ coordination sphere is defined by two N_{pyridyl} donors, three O_{nitrate} donors, and one N donor from a coordinated CH_3CN solvent molecule. The Cu–O(2) bond distance of $2.5394(17)$ Å is significantly longer than the rest of the Cu–O bond distances,¹⁶ whereas the Cu–N(5) distance of $2.505(17)$ Å is indicative of a

(16) Hagrman, D.; Hammond, R. P.; Haushalter, R.; Zubieta, J. *Chem. Mater.* **1999**, *10*, 2091.

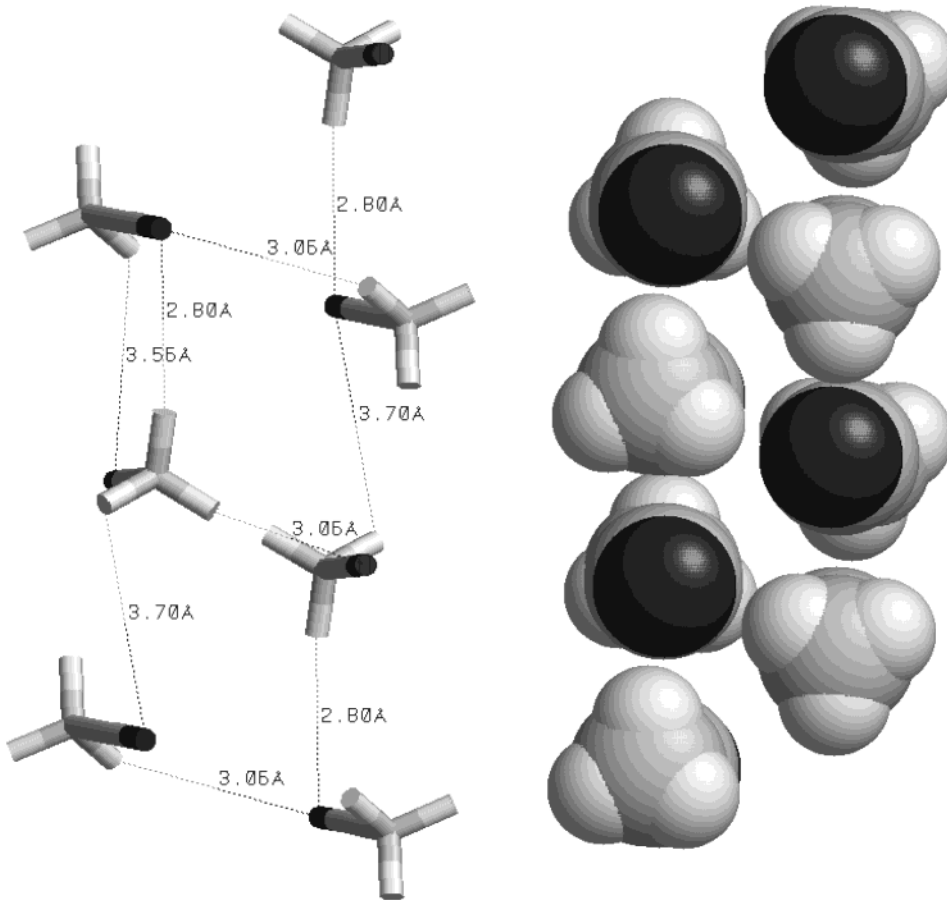


Figure 9. Packing diagram of CH_3CN guest molecules in **2**.

Table 8. Hydrogen Bonds for 3 [Å and deg]^a

D–H…A	<i>d</i> (D–H)	<i>d</i> (H…A)	<i>d</i> (D…A)	\angle (DHA)
O(2)–H(2A)…O(6) ^{#1}	0.80(2)	1.98(2)	2.7619(15)	166(2)
O(2)–H(2B)…N(2) ^{#2}	0.76(2)	2.12(2)	2.8572(16)	165.5(19)
O(3)–H(3A)…O(9) ^{#3}	0.84(2)	1.87(2)	2.7104(17)	173(2)
O(3)–H(3B)…N(3) ^{#2}	0.79(2)	2.10(2)	2.8606(18)	162.6(19)
O(4)–H(4A)…O(9) ^{#4}	0.80(2)	2.00(2)	2.7639(17)	161(2)
O(4)–H(4B)…O(10)	0.84(2)	1.94(2)	2.7684(16)	171(2)

^a Symmetry transformations used to generate equivalent atoms: #1, $-x + 1, -y + 1, -z + 1$; #2, $-x + 1, -y + 1, -z$; #3, $-x + 2, y + \frac{1}{2}, -z + \frac{1}{2}$; #4, $x, -y + \frac{1}{2}, z + \frac{1}{2}$.

weak Cu–CH₃CN interaction. It is not clear why the Zn(II) center in compound **3** did not coordinate to the CH₃CN guest molecules while Cu(II) in compound **4** did. In the solid state, Cu(II)-containing macrocycles stack together along the crystallographic *a* axis by inter-ring π – π (3.4 Å) interactions to generate squarelike channels (crystallographic dimensions, ca. 7.6 \times 7.5 Å²), in which the CH₃CN guest molecules are located (Figure 13). No strong hydrogen-bonding interactions have been found, although some weak inter-ring C–H…O hydrogen bonds exist.

The field of designing and synthesizing metal-containing supramolecular macrocycles, especially squarelike compounds, is currently very active.¹⁷ As we know, most of them are generated from 4d or 5d metals such as Pt, Pd, and Re. Metal-containing supramolecular squarelike assemblies generated from 3d metals¹⁸

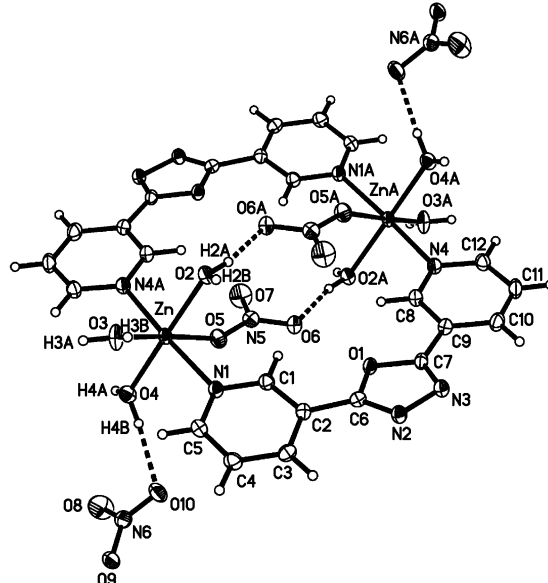


Figure 10. ORTEP figure of **3** with 50% probability ellipsoids.

and oxadiazole-containing ligands are quite rare. Compounds **3** and **4** described herein are soluble in both water and common organic solvents, such as CH₃CN and THF, which is an additional remarkable and useful feature for these two interesting compounds. It is worth pointing out that the coordination chemistry of the L₂ ligand is versatile. It can coordinate metal ions

(17) Leininger, S.; Olenyuk, B.; Stang, P. J. *Chem. Rev.* **2000**, *100*, 813 and references therein.

(18) Stang, P. J.; Persky, N. E. *J. Chem. Soc., Chem. Commun.* **1997**, 77.

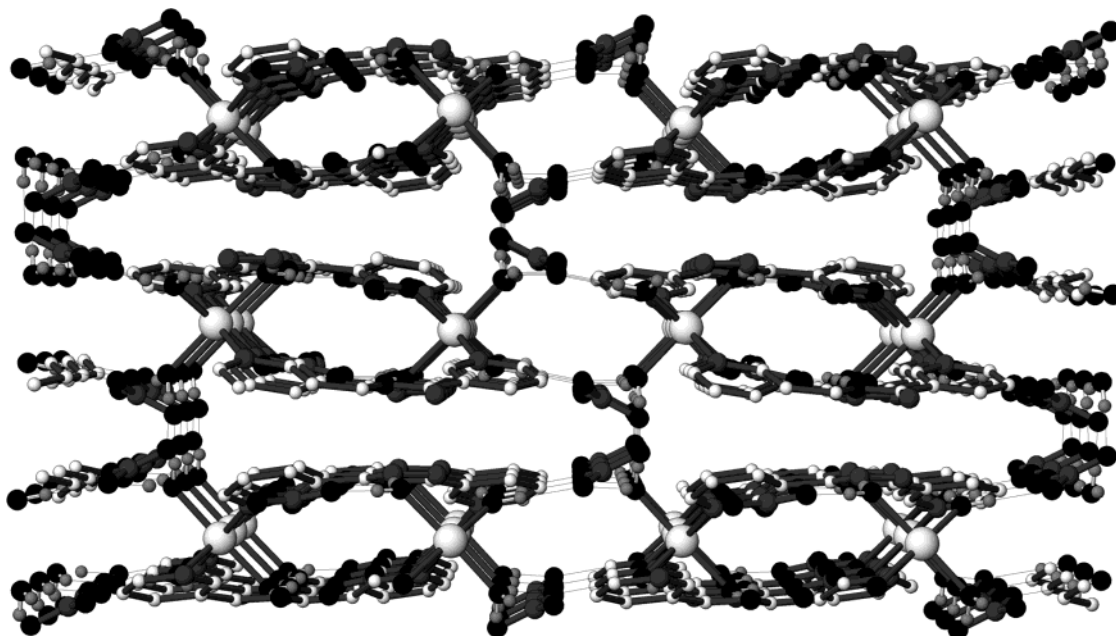


Figure 11. H-bonded three-dimensional network of **3** (view down the *c* axis).

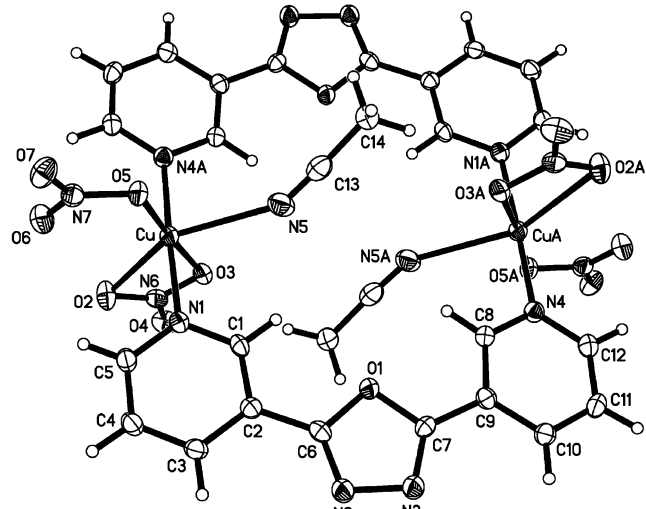


Figure 12. ORTEP figure of **4** with 50% probability ellipsoids.

in either the *cis* or *trans* configuration that was found in our previous studies.⁶ For example, the *cis*-L2 was found in coordination polymers $\text{Cu}_2(\text{OAc})_2(\text{L2})$ ^{6a} and $\text{Cu}(\text{hfacac})_2(\text{L2})$,^{6c} while the *trans*-L2 was found in coordination polymers $\text{Cu}(\text{L2})_2(\text{ClO}_4)_2$ and $[\text{Cu}(\text{L2})(\text{H}_2\text{O})](\text{SO}_4) \cdot 2.75\text{H}_2\text{O}$.^{6c} However, no bimetallic macrocyclic complexes were obtained in our previous studies, probably because of the templating effects of different counterions as well as solvent molecules.

Luminescent Properties of **3 and **4**.** Mixed inorganic–organic hybrid supramolecular coordination compounds have been investigated for fluorescence properties and for potential applications as light-emitting diodes (LEDs).¹⁹ Owing to the higher thermal stability of inorganic–organic coordination polymers and the ability of affecting the emission wavelength of organic materials, syntheses of inorganic–organic coordination supramolecular complexes by the judicious choice of

organic spacers and transition-metal centers can be an efficient method for obtaining new types of electroluminescent materials.²⁰ The luminescent properties of both compounds **3** and **4** were investigated in CH_3CN and solid state. The fluorescence spectra of compounds L2, **3**, and **4** in CH_3CN are shown in Figure 14a. As shown in Figure 14a, L2 exhibits two emission maxima at 360 and 381 nm. The emission spectrum of **3** in CH_3CN is red-shifted to 401 nm. The emission of **4** in CH_3CN is red-shifted to 384 nm, with a second, less intense band present at 368 nm. In the solid state, excimer formation of L2, **3**, and **4** is observed, as shown in Figure 14b; L2 exhibits one emission maximum at 360 nm. The emission of **3** is red-shifted to 367 nm. The emission of **4** is red-shifted to 380 nm, with a second, less intense band present at 420 nm. However, no enhancement of the fluorescence intensities is realized in both compounds **3** and **4**. The emission color of the free L2 was significantly affected by its incorporation into the M(II)-containing (M = Cu and Zn) supramolecular compounds **3** and **4**, as evidenced by the shift in the emission in the solid state. Reasonably, the presence of the intervening Zn(II) and Cu(II) atoms, which exert an electron-withdrawing effect as a consequence of their +2 charge and attached NO_3^- , has a significant influence on the fluorescent properties of the ligand. We have started to alter the fluorescent oxadiazole-containing organic spacer by modifying the length both to change the luminescent properties and to affect the structures of coordination polymers or supramolecular complexes that form. This should, presumably, lead to new, tunable, luminescent materials.

Conclusions

This study demonstrates that the oxadiazole-containing rigid organic ligands L1 and L2 are capable of

(19) (a) Altmann, M.; Bunz, U. H. F. *Angew. Chem.* **1995**, *34*, 569. (b) Bunz, U. H. F. *Chem. Rev.* **2000**, *100*, 1605.

(20) (a) Ciurton, D. M.; Pschirer, N. G.; Smith, M. D.; Bunz, U. H. F.; zur Loya, H.-C. *Chem. Mater.* **2001**, *13*, 2743. (b) Cariati, E.; Bu, X.; Ford, P. C. *Chem. Mater.* **2000**, *12*, 3385. (c) Würthner, F.; Sautter, A. *Chem. Commun.* **2000**, 445.

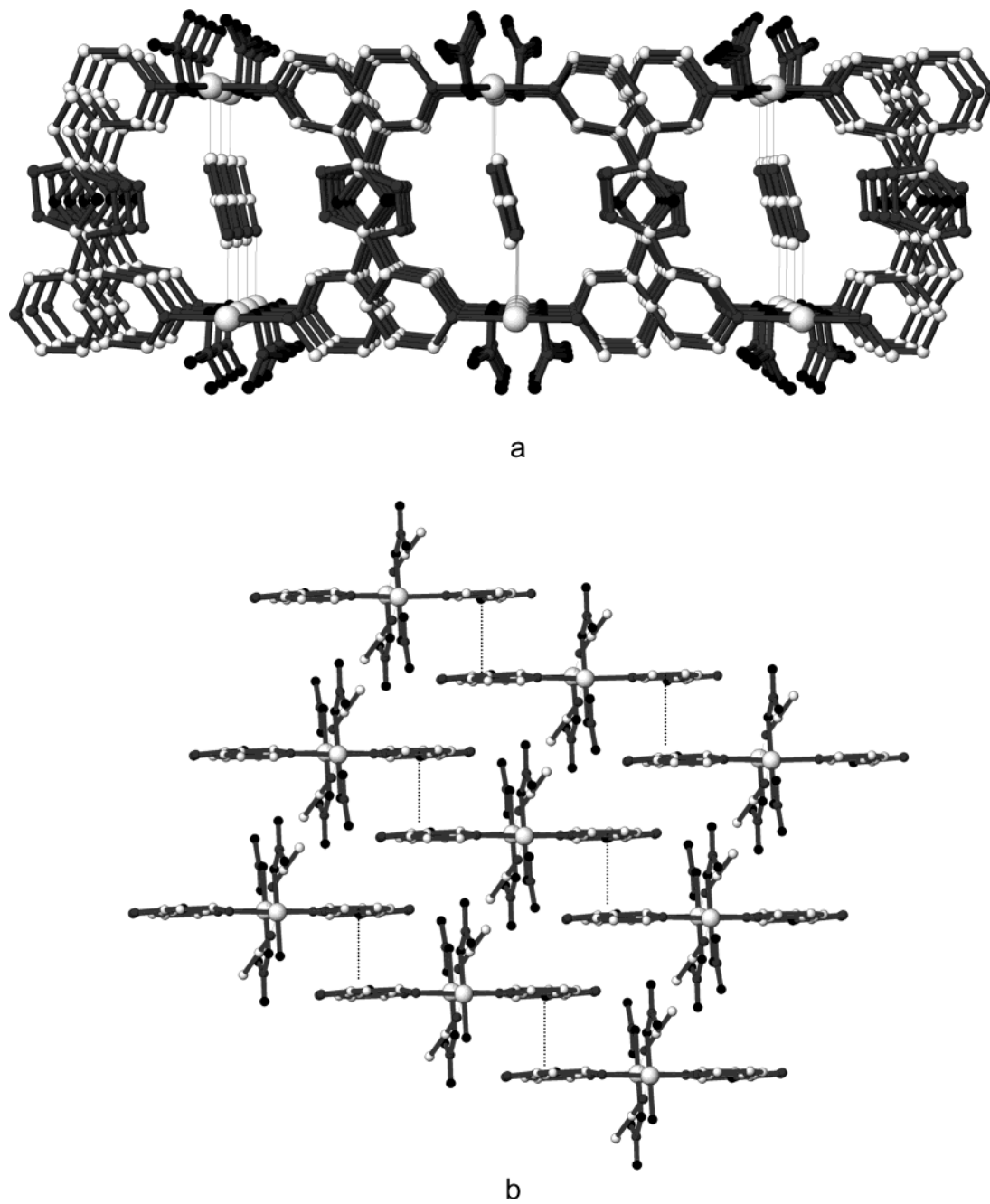


Figure 13. (a) Crystal packing of **4** (view down the *a* axis). (b) π - π stacking interactions found in **4** (view down the *c* axis).

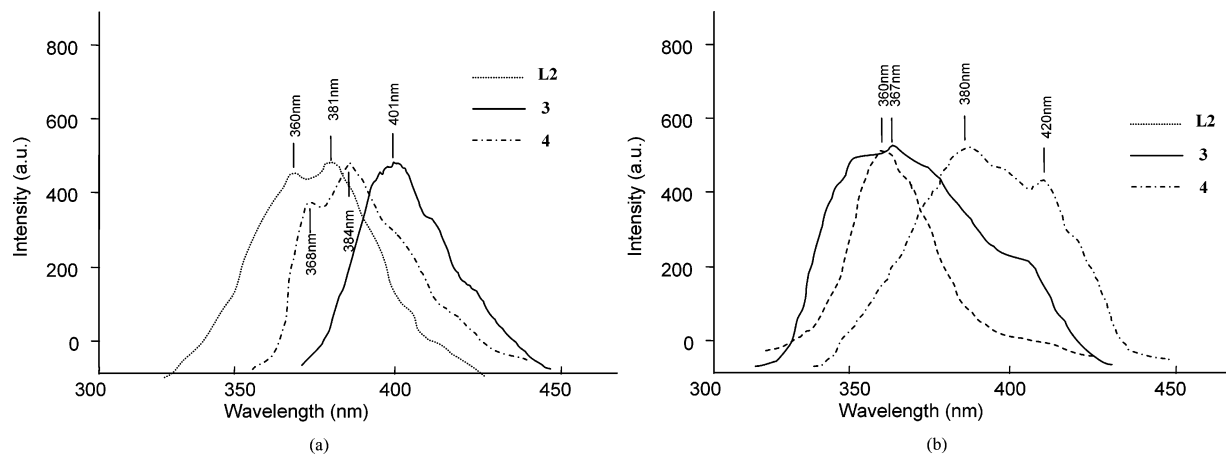


Figure 14. (a) Photoinduced emission spectra of **L2**, **3**, and **4** in CH_3CN at room temperature. (b) Photoinduced emission spectra of **L2**, **3**, and **4** in the solid state at room temperature.

coordinating transition-metal ions with N_{pyridyl} donors to generate both polymeric and molecular compounds. Two new coordination polymers (**1** and **2**) and two new bimetallic macrocyclic supramolecular complexes (**3** and **4**) were synthesized from solution reactions of L1 and L2 with inorganic M(II) (M = Zn and Cu) salts. The relative orientation of the nitrogen donors on the pyridyl rings and the five-membered oxadiazole spacing in L1 and L2 resulted in unusual building blocks, leading to the construction of polymeric motifs which have not been obtained using linear rigid bidentate organic ligands, such as 4,4'-bipyridine or similar organic spacers. We are currently extending this result by preparing new oxadiazole-containing ligands of this type containing different coordination functional groups and having different orientations of the nitrogen donors on the pyridyl rings. We anticipate that this new type of

organic ligand will result in a variety of new coordination polymers and supramolecular complexes with novel polymeric patterns and interesting physical properties.

Acknowledgment. We are grateful for financial support from the National Natural Science Foundation of China (No. 20174023 and 60047001), Shandong Natural Science Foundation (No. Z2001B01), and Young Scientists Funding of Shandong Province of P.R. China. We also are thankful for financial support from Starting Funding of China for overseas scholars, Shandong Normal University, and Open Foundation of State Key Lab of Crystal Materials. H.-C.z.L. gratefully acknowledges support from the NSF through Grant DMR 0134156.

CM030037T